

## Supporting Information

### Azulene-porphyrin based covalent organic frameworks for applications in second order nonlinear optics

*Jiao-Jiao Deng<sup>a</sup>, You-Zhao Lan<sup>b\*</sup>, Cui-Cui Yang<sup>c\*</sup>, Wei Quan Tian<sup>a\*</sup>*

a: Chongqing Key Laboratory of Chemical Theory and Mechanism, College of Chemistry and Chemical Engineering, Chongqing University, Huxi Campus, Chongqing 401331, P. R. China

b: Key Laboratory of the Ministry of Education for Advanced Catalysis Materials, College of Chemistry and Life Sciences, Zhejiang Normal University, Jinhua, Zhejiang, 321004, P. R. China

c: School of Mathematical Science, Chongqing University of Technology, Huaxi Campus, Chongqing 400054, P. R. China

\*Corresponding author: [tianwq@cqu.edu.cn](mailto:tianwq@cqu.edu.cn); [lyzhao@zjnu.cn](mailto:lyzhao@zjnu.cn); [yangcc@cqut.edu.cn](mailto:yangcc@cqut.edu.cn)

## Supporting Information list:

**Figure S1** The diagram of  $|\chi_{xxx}^{(2)}(\omega)|$  for PoBe varying with the density of  $k$  grid points (with a fixed number of 80 empty bands) and the number of empty bands (with a fixed  $k$  grid of  $6 \times 6 \times 1$ ).

**Figure S2** Band structure and DOS of (a) Zn-PoBe, (b) Zn-PoAz, (c) Zn-PoAzD, (d) Zn-PoAzN, (e) Zn-PoAzNN and (f) Zn-PoAzBN predicted by HLE17.

**Figure S3** 3D charge density distribution of (a) Zn-PoBe, (b) Zn-PoAz, (c) Zn-PoAzD, (d) Zn-PoAzN, (e) Zn-PoAzN2, (f) Zn-PoAzB, (g) Zn-Po2Az and (h) Zn-Po2AzB predicted by HLE17, isosurface=0.0005 C/m<sup>3</sup>.

**Figure S4** Frequency dependency of two main components (a)  $|\chi_{xxx}^{(2)}(\omega)|$  and (b)  $|\chi_{yyy}^{(2)}(\omega)|$  in the SHG response of the designed COFs (in  $10^{-7}$  esu).

**Figure S5** Band structure and DOS of (a) PoBeD, (b) PoBeN, (c) PoBeNN and (d) PoBeBN predicted by HLE17.

**Figure S6** Planarity of other structures,  $\theta$  denotes the torsional angle.

**Figure S7** SHG Frequency dependency of (a) PoAzNN and (b) Zn-Po2AzN. From bottom to top, each subplot represents the imaginary part of the dielectric function, the frequency dependency of  $Im[\chi_{yyy}^{(2)}(\omega)]$  decomposed into  $\omega$  and  $2\omega$  terms, and the frequency dependency of decomposed  $Im[\chi_{yyy}^{(2)}(\omega)]$  as a function of input photon energy.

**Figure S8** SHG Frequency dependency of Po2AzN. From bottom to top, each subplot represents the part of the dielectric function, the frequency dependency of  $Re[\chi_{yyy}^{(2)}(\omega)]$  decomposed into  $\omega$  and  $2\omega$  terms, and the frequency dependency of decomposed  $Re[\chi_{yyy}^{(2)}(\omega)]$  as a function of input photon energy.

**Figure S9** Frequency dispersion of the decomposed  $Im[\chi_{yyy}^{(2)}(\omega)]$  of (a) PoAzNN and (b) Zn-Po2AzN into 2-bands and 3-bands terms.

**Figure S10** SHG Frequency dependency of (a) PoBe, (b) PoAz, (c) PoAzD, (d) PoAzN, (e) PoAzNN and (f) PoAzBN. From bottom to top, each subplot represents the real part of the dielectric function, the frequency dependency of  $Re[\chi_{yyy}^{(2)}(\omega)]$  decomposed into  $\omega$  and  $2\omega$  terms, and the frequency dependency of decomposed  $Re[\chi_{yyy}^{(2)}(\omega)]$  as a function of input photon energy.

**Figure S11** SHG Frequency dependency of (a) PoBe, (b) PoAz, (c) PoAzD, (d) PoAzN, (e) PoAzNN and (f) PoAzBN. From bottom to top, each subplot represents the imaginary part of the dielectric function, the frequency dependency of  $Im[\chi_{yyy}^{(2)}(\omega)]$  decomposed into  $\omega$  and  $2\omega$  terms, and the frequency dependency of decomposed  $Im[\chi_{yyy}^{(2)}(\omega)]$  as a function of input photon energy.

**Figure S12** SHG Frequency dependency of (a) Zn-PoBe, (b) Zn-PoAz, (c) Zn-PoAzD, (d) Zn-PoAzN, (e) Zn-PoAzNN and (f) Zn-PoAzBN. From bottom to top, each subplot represents the real part of the dielectric function, the frequency dependency of  $Re[\chi_{yyy}^{(2)}(\omega)]$  decomposed into  $\omega$  and  $2\omega$  terms, and the frequency dependency of decomposed  $Re[\chi_{yyy}^{(2)}(\omega)]$  as a function of input photon energy.

**Figure S13** SHG Frequency dependency of (a) Zn-PoBe, (b) Zn-PoAz, (c) Zn-PoAzD, (d) Zn-PoAzN, (e) Zn-PoAzNN and (f) Zn-PoAzBN. From bottom to top, each subplot represents the imaginary part of the dielectric function, the frequency dependency of  $Im[\chi_{yyy}^{(2)}(\omega)]$  decomposed into  $\omega$  and  $2\omega$  terms, and the frequency dependency of decomposed  $Im[\chi_{yyy}^{(2)}(\omega)]$  as a function of input photon energy.

**Figure S14** Frequency dispersion of the decomposed  $Re[\chi_{yyy}^{(2)}(\omega)]$  of (a) PoBe, (b) PoAz, (c) PoAzD, (d) PoAzN, (e) PoAzNN and (f) PoAzBN into 2-bands and 3-bands terms.

**Figure S15** Frequency dispersion of the decomposed  $Im[\chi_{yyy}^{(2)}(\omega)]$  of (a) PoBe, (b) PoAz, (c) PoAzD, (d) PoAzN, (e) PoAzNN and (f) PoAzBN into 2-bands and 3-bands terms.

**Figure S16** Frequency dispersion of the decomposed  $Re[\chi_{yyy}^{(2)}(\omega)]$  of (a) Zn-PoBe, (b) Zn-PoAz, (c) Zn-PoAzD, (d) Zn-PoAzN, (e) Zn-PoAzNN and (f) Zn-PoAzBN into 2-bands and 3-bands terms.

**Figure S17** Frequency dispersion of the decomposed  $Im[\chi_{yyy}^{(2)}(\omega)]$  of (a) Zn-PoBe, (b) Zn-PoAz, (c) Zn-PoAzD, (d) Zn-PoAzN, (e) Zn-PoAzNN and (f) Zn-PoAzBN into 2-bands and 3-bands terms.

**Table S1** Electronic properties of selected systems predicted with HLE17 and PBE.

**Table S2**  $\chi_{ijk}^{(2)}$  along the  $x$ -direction at static limit (in pm/V).

**Table S3**  $\chi_{ijk}^{(2)}$  along the  $y$ -direction at static limit (in pm/V).

**Table S4**  $\chi_{ijk}^{(2)}$  along the  $z$ -direction at static limit (in pm/V).

**Table S5** The electronic properties of molecules predicted with B3LYP/6-31G (d, p).

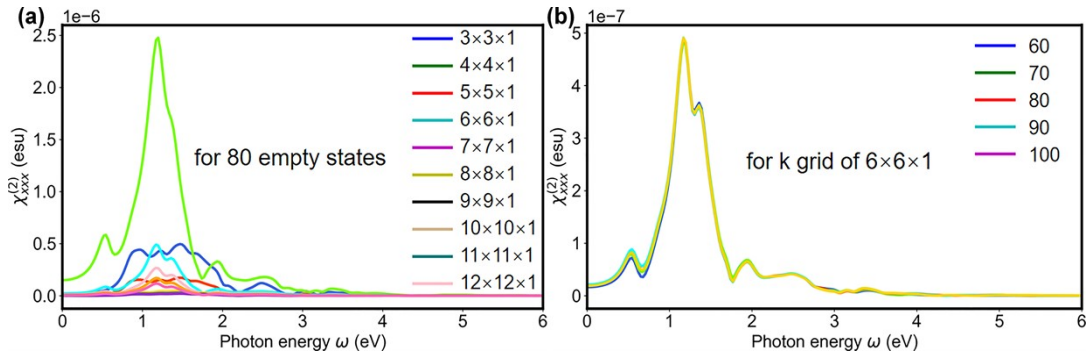


**Figure S1** The diagram of  $|\chi_{xxx}^{(2)}(\omega)|$  for PoBe varying with the density of k grid points (with a fixed number of 80 empty bands) and the number of empty bands (with a fixed k grid of  $6 \times 6 \times 1$ ).

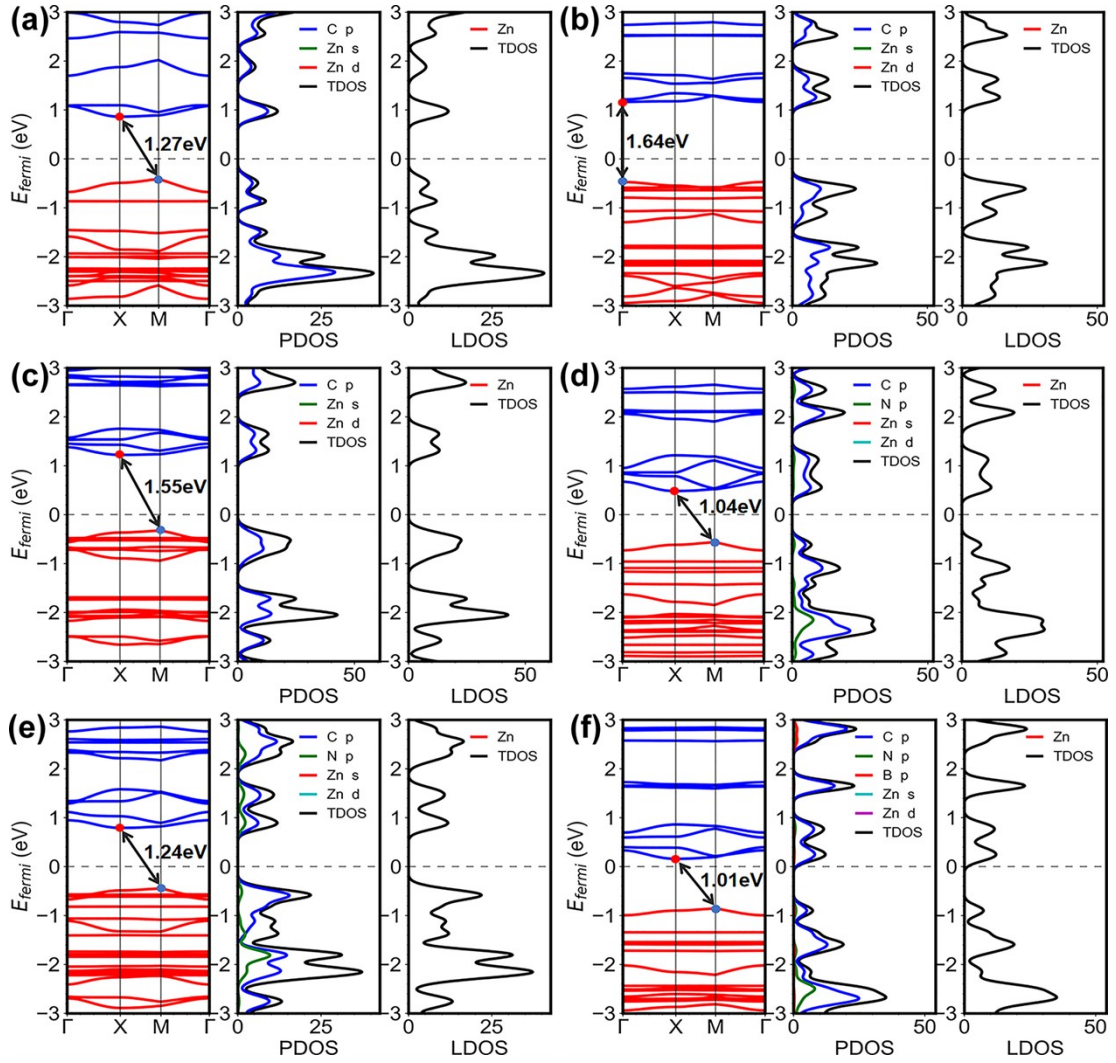


**Figure S2** Band structure and DOS of (a) Zn-PoBe, (b) Zn-PoAz, (c) Zn-PoAzD, (d) Zn-PoAzN, (e) Zn-PoAzNN and (f) Zn-PoAzBN predicted by HLE17.

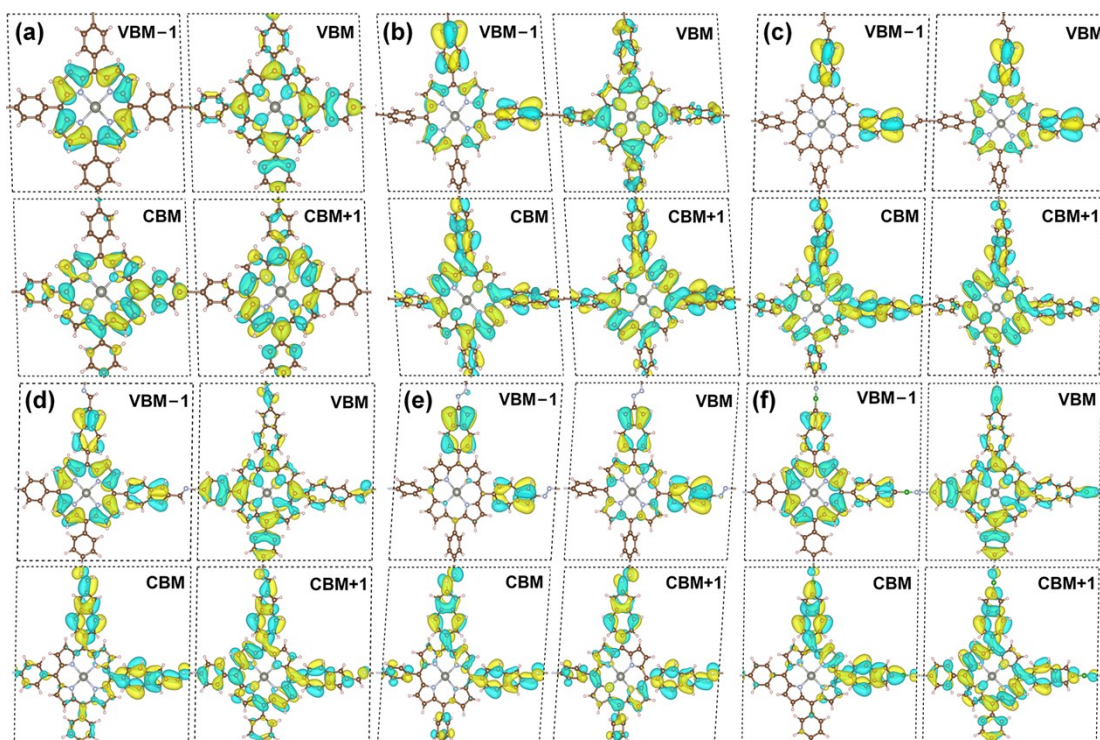


**Figure S3** 3D charge density distribution of (a) Zn-PoBe, (b) Zn-PoAz, (c) Zn-PoAzD, (d) Zn-PoAzN, (e) Zn-PoAzN2, (f) Zn-PoAzB, (g) Zn-Po2Az and (h) Zn-Po2AzB predicted by HLE17, isosurface=0.0005 C/m<sup>3</sup>.

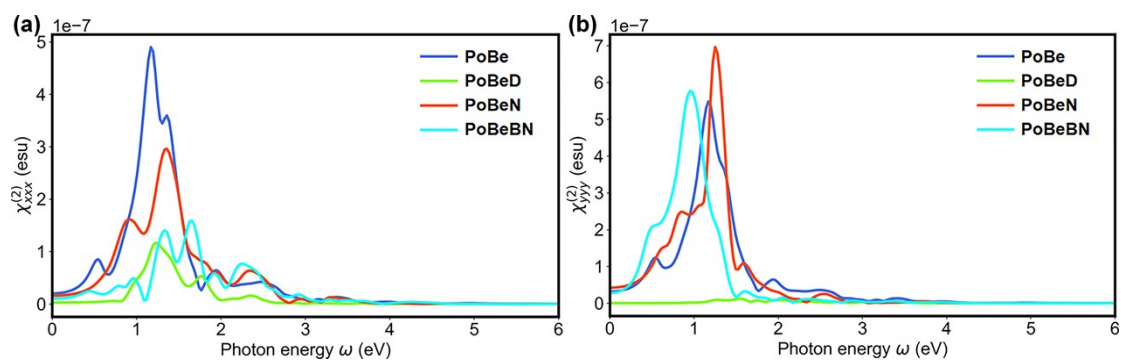


**Figure S4** Frequency dependency of two main components (a)  $|\chi_{xxx}^{(2)}(\omega)|$  and (b)  $|\chi_{yyy}^{(2)}(\omega)|$  in the SHG response of the designed COFs (in  $10^{-7}$  esu).

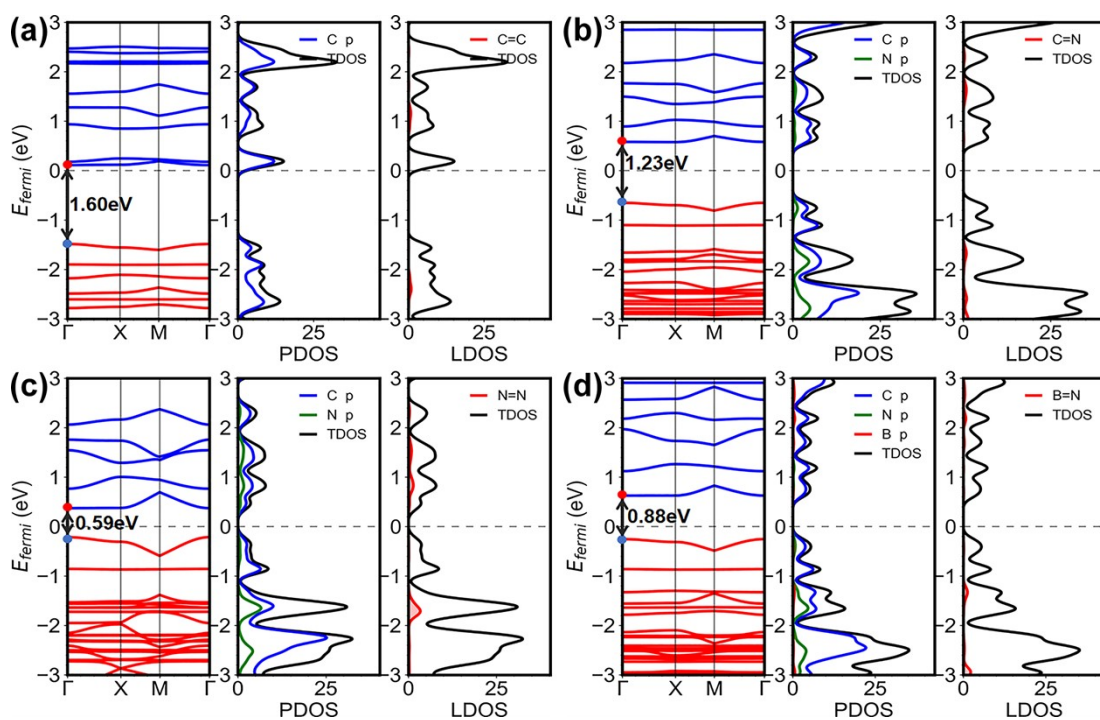


**Figure S5** Band structure and DOS of (a) PoBeD, (b) PoBeN, (c) PoBeNN and (d) PoBeBN predicted by HLE17.

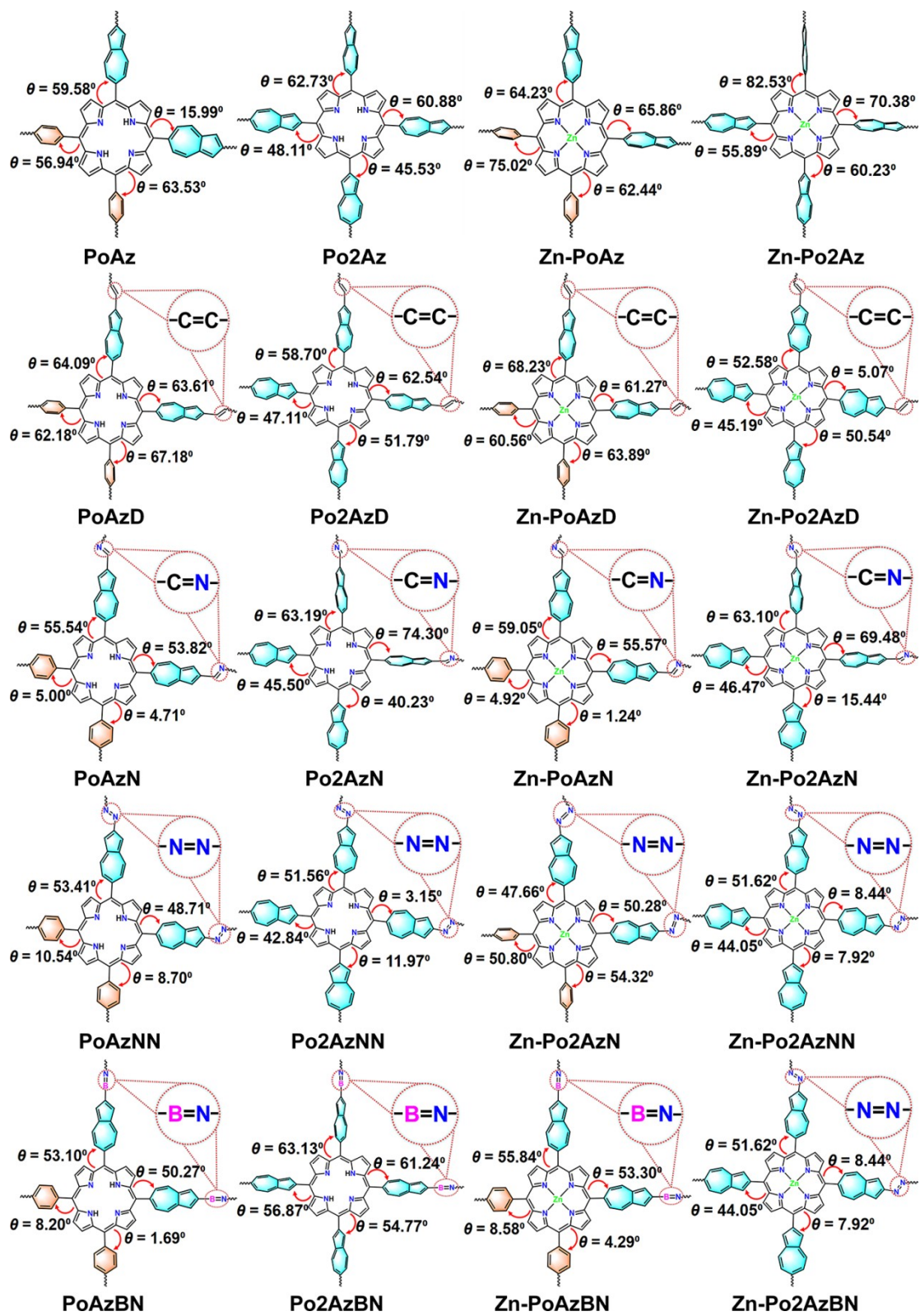
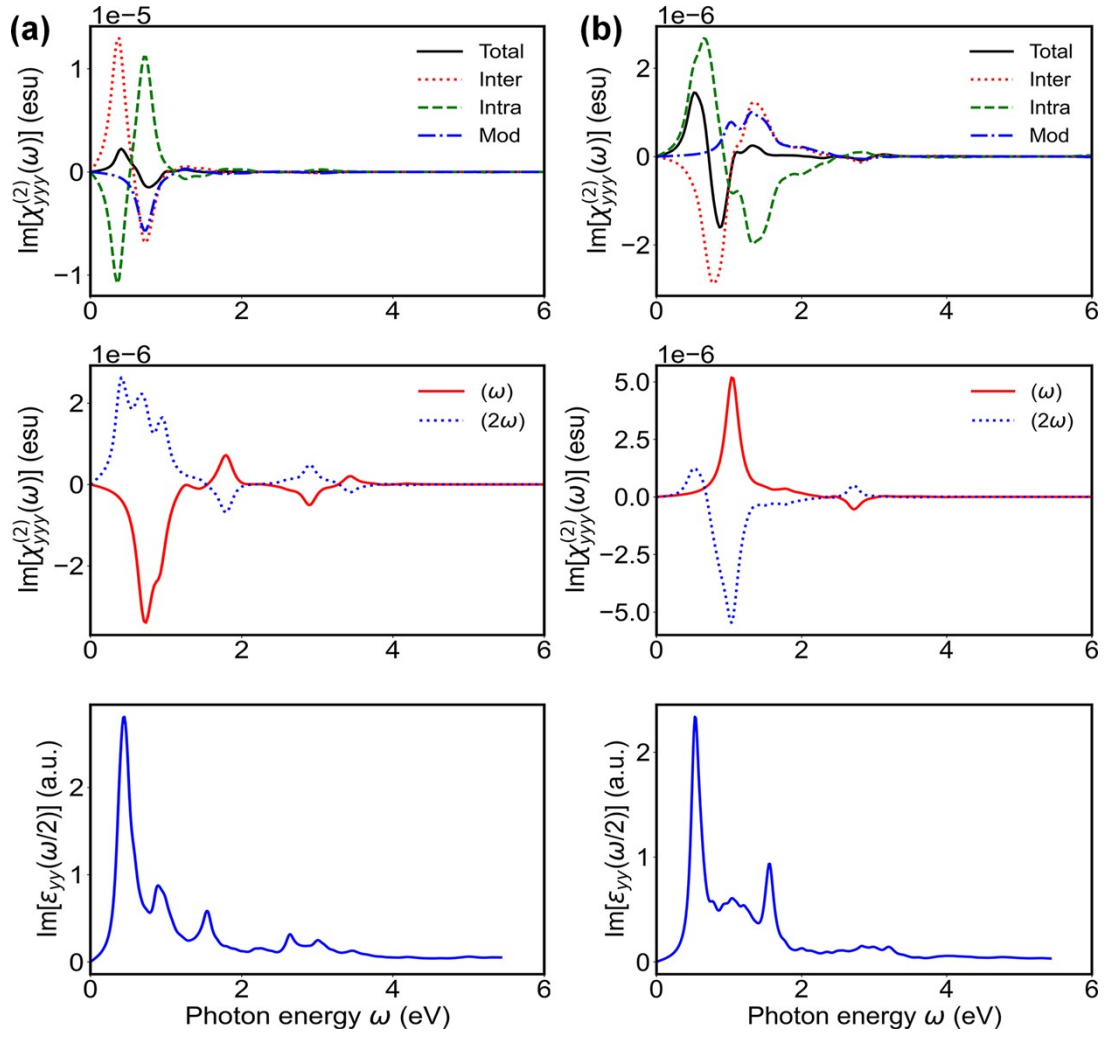
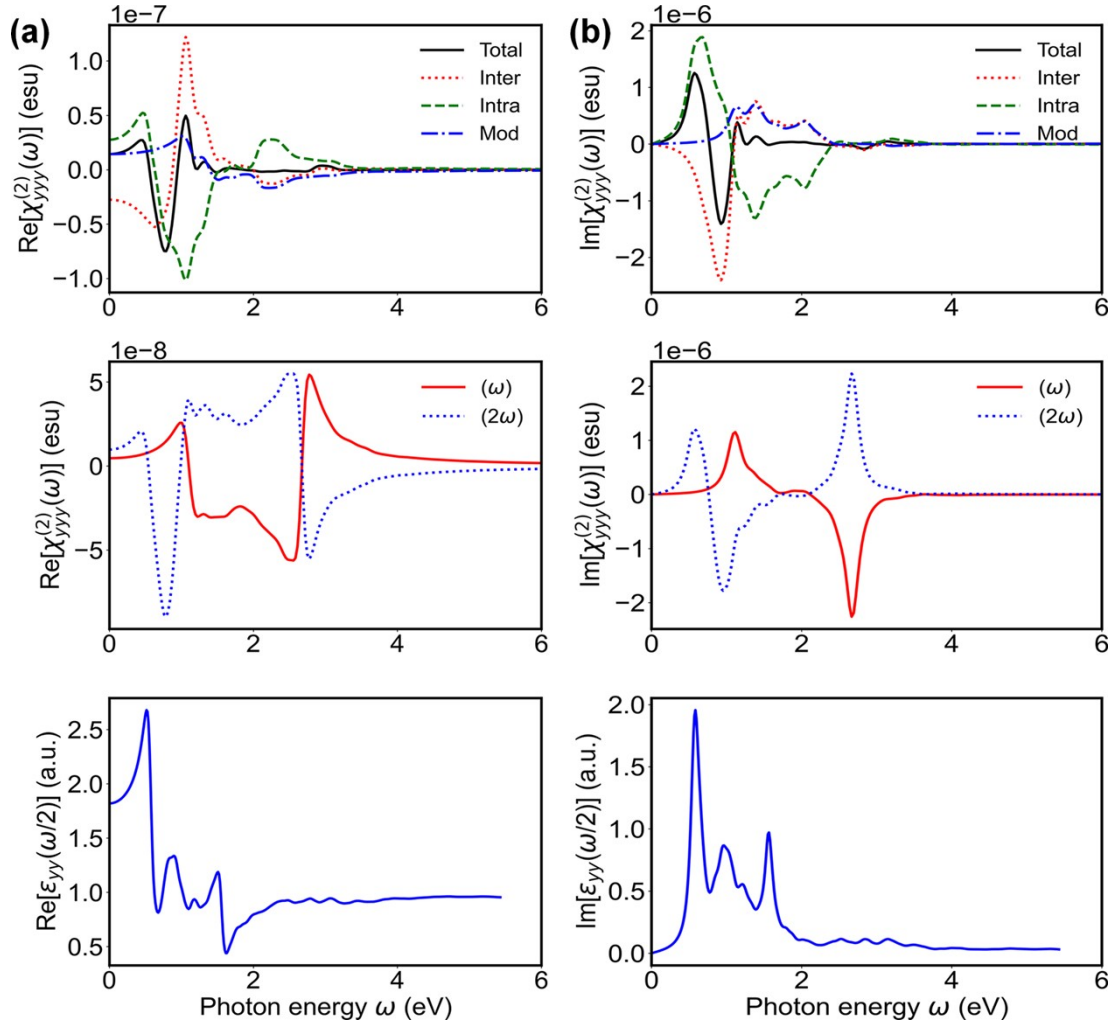


Figure S6 Planarity of other structures,  $\theta$  denotes the torsional angle.



**Figure S7** SHG Frequency dependency of (a) PoAzNN and (b) Zn-Po2AzN. From bottom to top, each subplot represents the imaginary part of the dielectric function, the frequency dependency of  $\text{Im}[\chi_{yyy}^{(2)}(\omega)]$  decomposed into  $\omega$  and  $2\omega$  terms, and the frequency dependency of decomposed  $\text{Im}[\chi_{yyy}^{(2)}(\omega)]$  as a function of input photon energy.



**Figure S8** SHG Frequency dependency of Po2AzN. From bottom to top, each subplot represents the part of the dielectric function, the frequency dependency of  $Re[\chi_{yyy}^{(2)}(\omega)]$  decomposed into  $\omega$  and  $2\omega$  terms, and the frequency dependency of decomposed  $Re[\chi_{yyy}^{(2)}(\omega)]$  as a function of input photon energy.

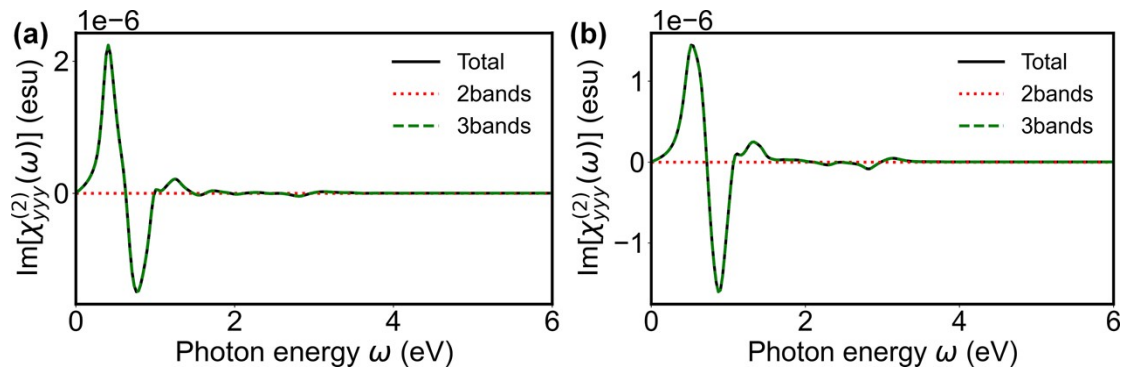


**Figure S9** Frequency dispersion of the decomposed  $Im[\chi_{yyy}^{(2)}(\omega)]$  of (a) PoAzNN and (b) Zn-Po2AzN into 2-bands and 3-bands terms.

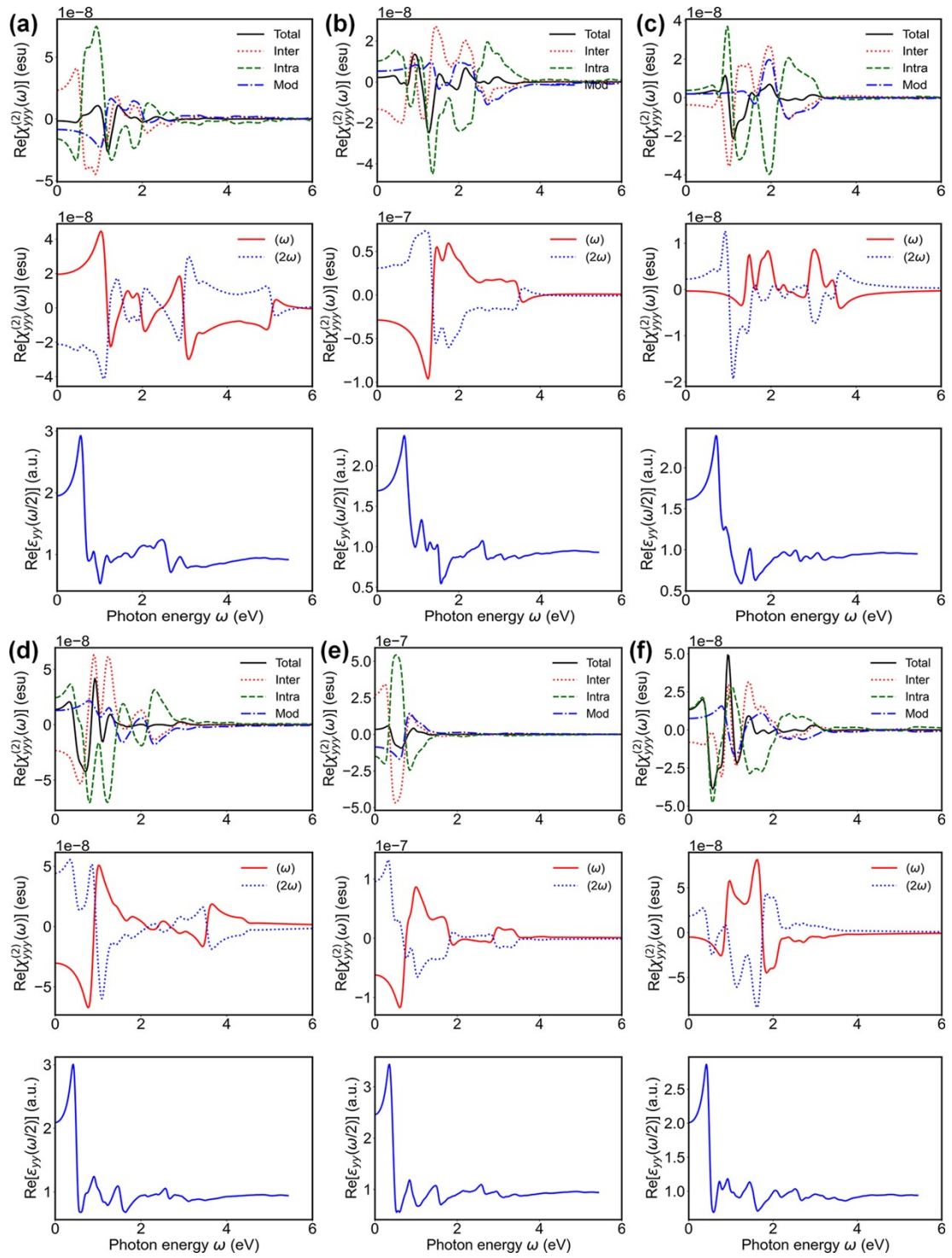


**Figure S10** SHG Frequency dependency of (a) PoBe, (b) PoAz, (c) PoAzD, (d) PoAzN, (e) PoAzNN and (f) PoAzBN. From bottom to top, each subplot represents the real part of the dielectric function, the frequency dependency of  $Re[\chi_{yyy}^{(2)}(\omega)]$  decomposed into  $\omega$  and  $2\omega$  terms, and the frequency dependency of decomposed  $Re[\chi_{yyy}^{(2)}(\omega)]$  as a function of input photon energy.

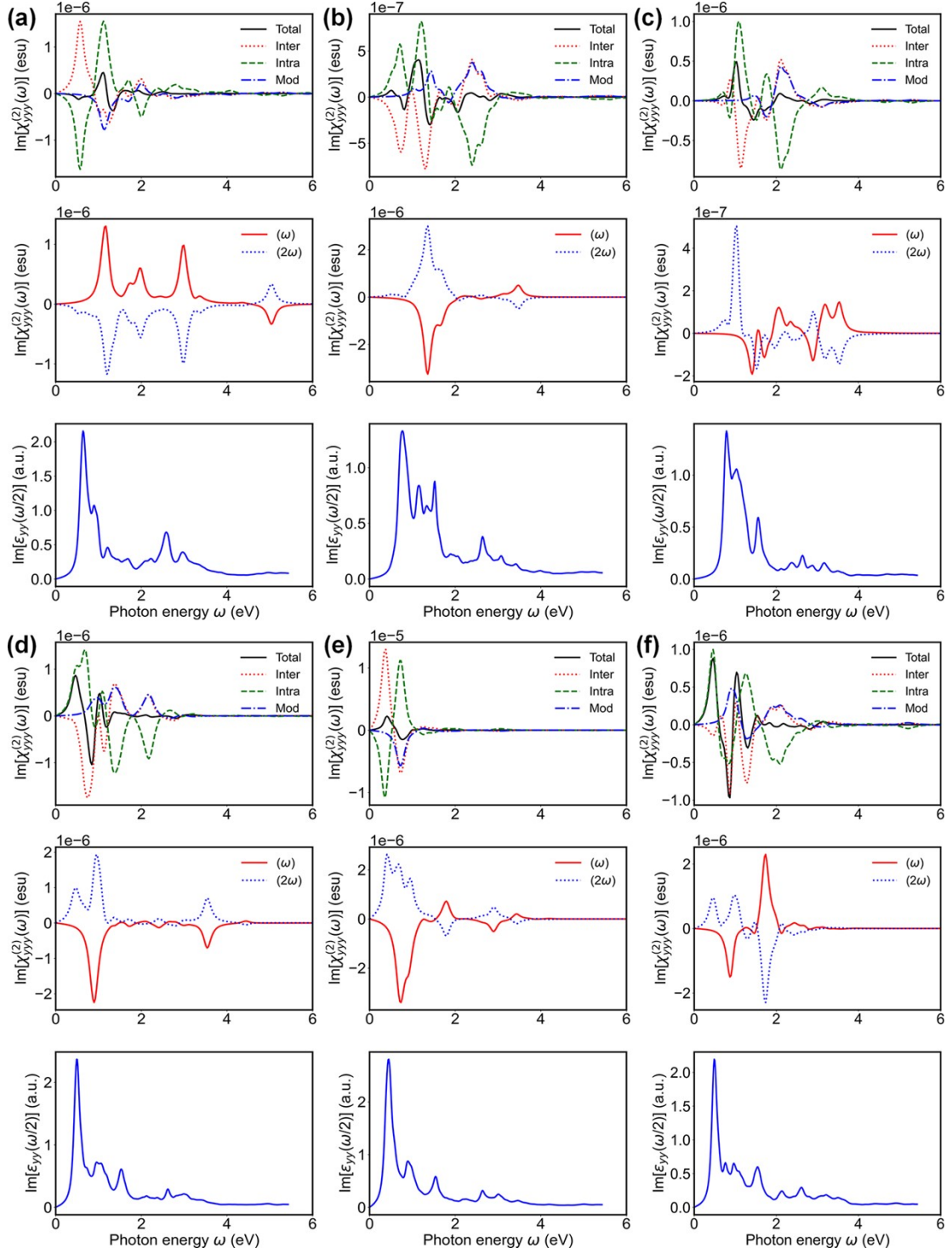


**Figure S11** SHG Frequency dependency of (a) PoBe, (b) PoAz, (c) PoAzD, (d) PoAzN, (e) PoAzNN and (f) PoAzBN. From bottom to top, each subplot represents the imaginary part of the dielectric function, the frequency dependency of  $Im[\chi_{yyy}^{(2)}(\omega)]$  decomposed into  $\omega$  and  $2\omega$  terms, and the frequency dependency of decomposed  $Im[\chi_{yyy}^{(2)}(\omega)]$  as a function of input photon energy.

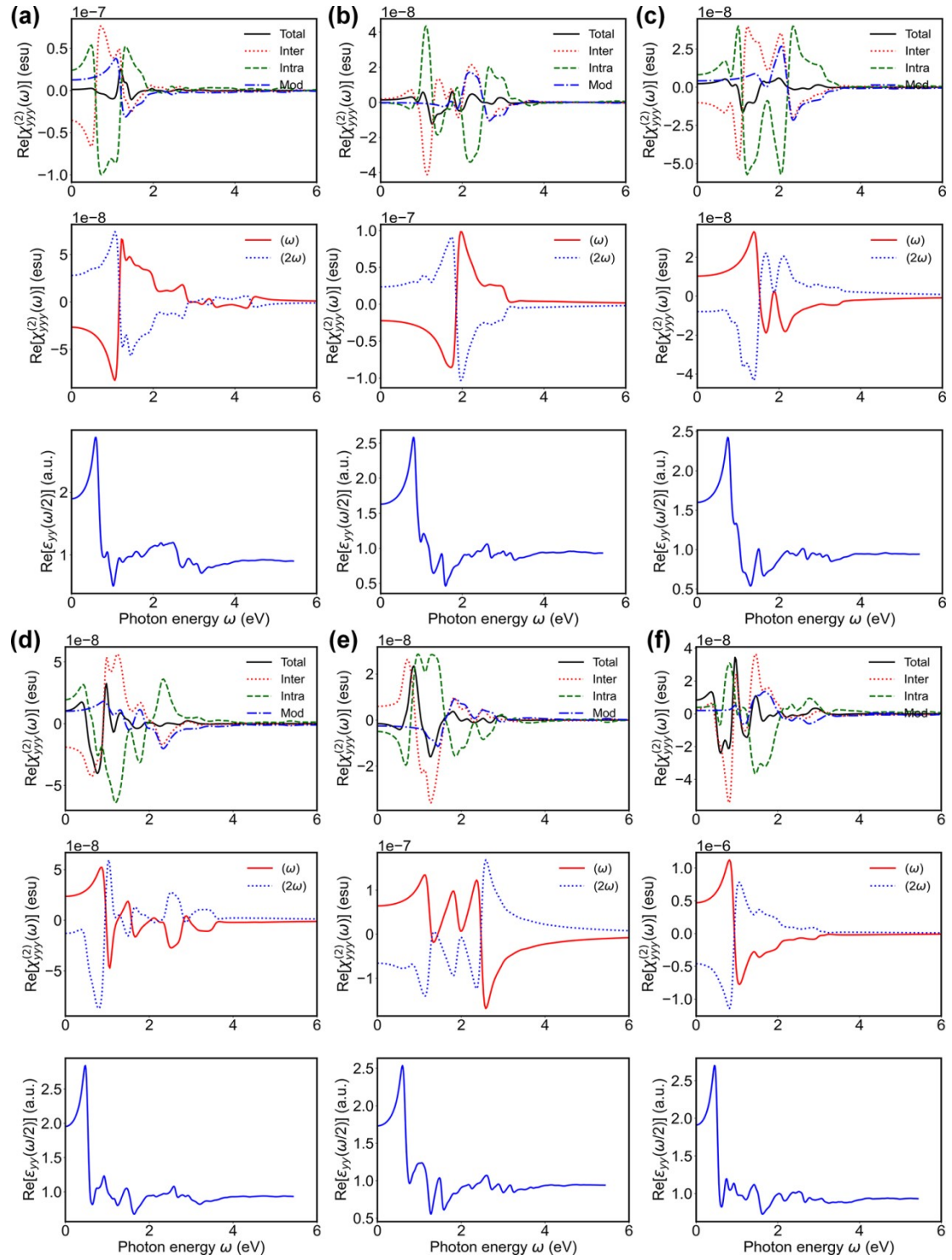


**Figure S12** SHG Frequency dependency of (a) Zn-PoBe, (b) Zn-PoAz, (c) Zn-PoAzD, (d) Zn-PoAzN, (e) Zn-PoAzNN and (f) Zn-PoAzBN. From bottom to top, each subplot represents the real part of the dielectric function, the frequency dependency of  $Re[\chi_{yyy}^{(2)}(\omega)]$  decomposed into  $\omega$  and  $2\omega$  terms, and the frequency dependency of decomposed  $Re[\chi_{yyy}^{(2)}(\omega)]$  as a function of input photon energy.

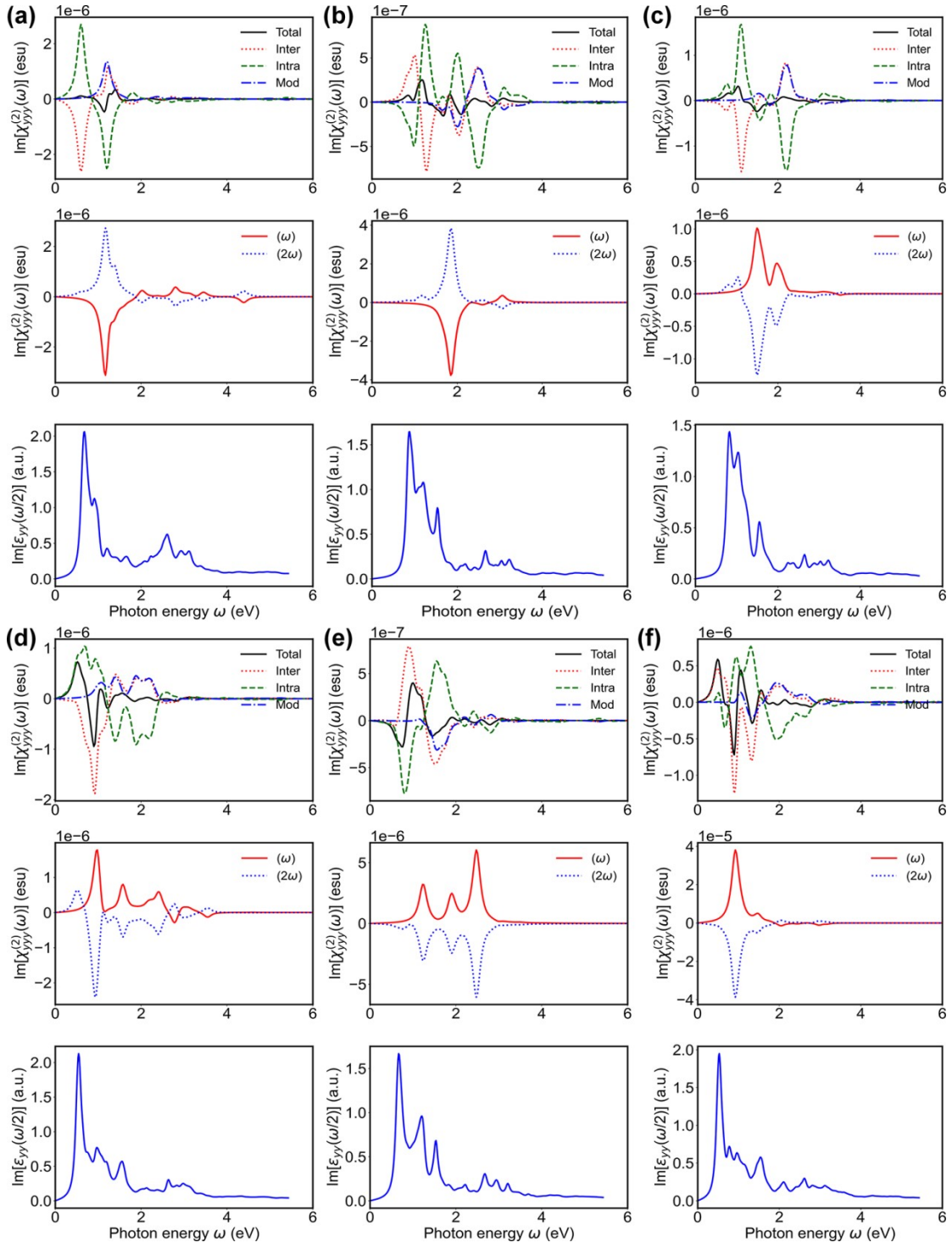


**Figure S13** SHG Frequency dependency of (a) Zn-PoBe, (b) Zn-PoAz, (c) Zn-PoAzD, (d) Zn-PoAzN, (e) Zn-PoAzNN and (f) Zn-PoAzBN. From bottom to top, each subplot represents the imaginary part of the dielectric function, the frequency dependency of  $Im[\chi_{yyy}^{(2)}(\omega)]$  decomposed into  $\omega$  and  $2\omega$  terms, and the frequency dependency of decomposed  $Im[\chi_{yyy}^{(2)}(\omega)]$  as a function of input photon energy.

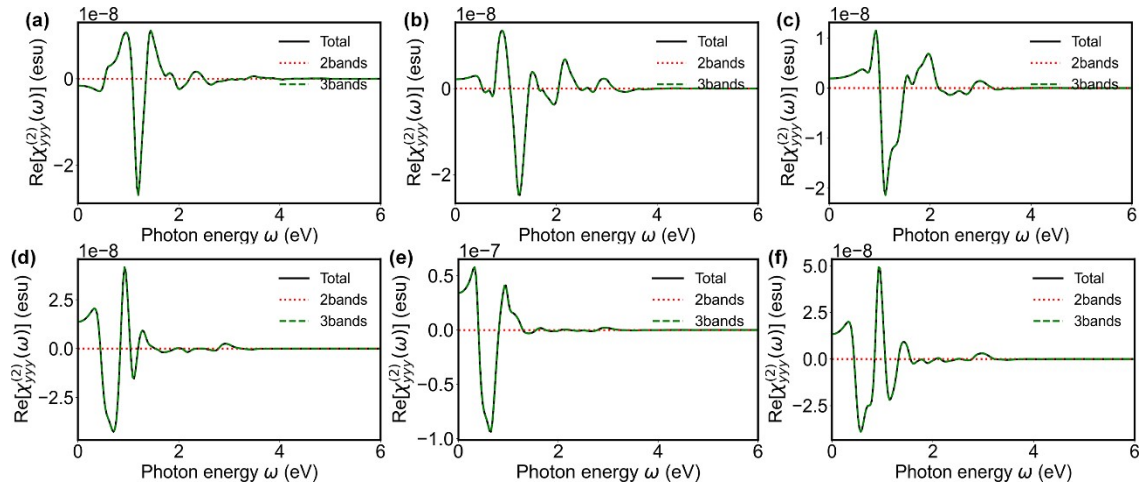


**Figure S14** Frequency dispersion of the decomposed  $Re[\chi_{yyy}^{(2)}(\omega)]$  of (a) PoBe, (b) PoAz, (c) PoAzD, (d) PoAzN, (e) PoAzNN and (f) PoAzBN into 2-bands and 3-bands terms.

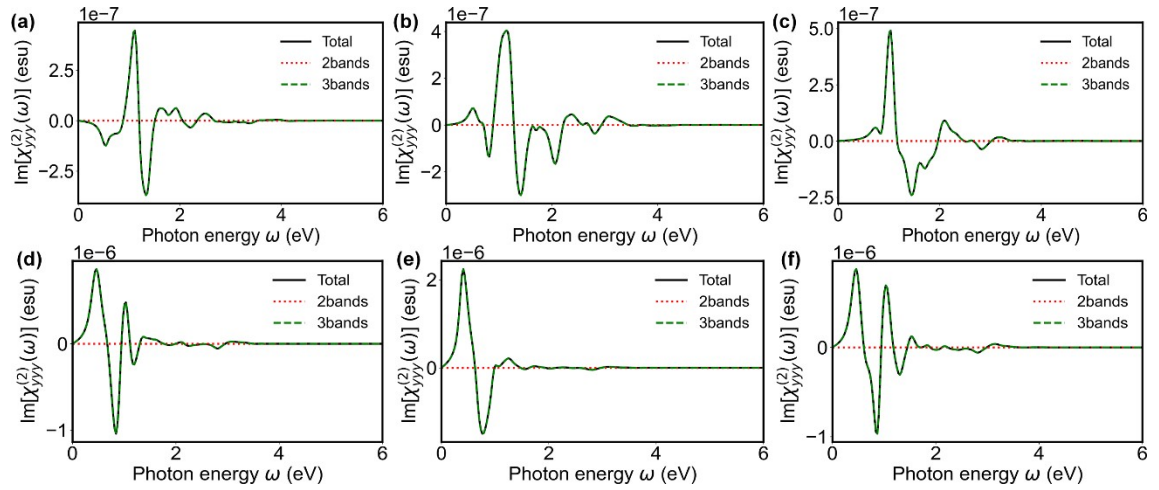


**Figure S15** Frequency dispersion of the decomposed  $Im[\chi_{yyy}^{(2)}(\omega)]$  of (a) PoBe, (b) PoAz, (c) PoAzD, (d) PoAzN, (e) PoAzNN and (f) PoAzBN into 2-bands and 3-bands terms.

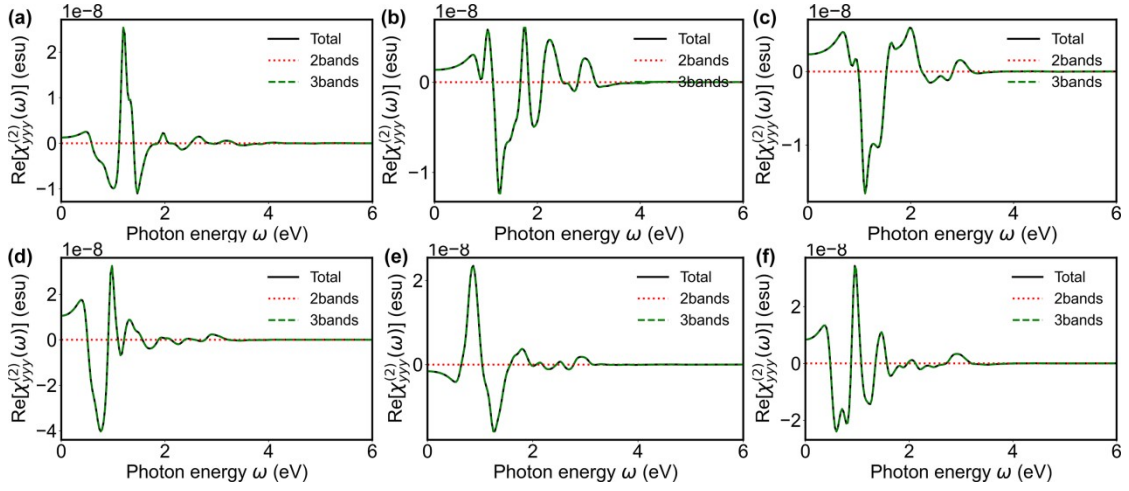


**Figure S16** Frequency dispersion of the decomposed  $Re[\chi_{yyy}^{(2)}(\omega)]$  of (a) Zn-PoBe, (b) Zn-PoAz, (c) Zn-PoAzD, (d) Zn-PoAzN, (e) Zn-PoAzNN and (f) Zn-PoAzBN into 2-bands and 3-bands terms.

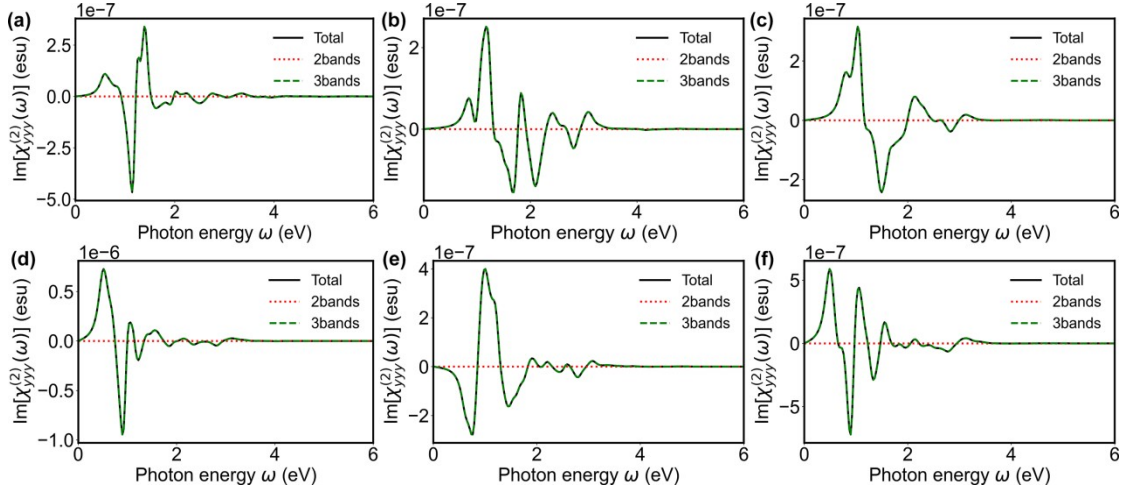


**Figure S17** Frequency dispersion of the decomposed  $Im[\chi_{yyy}^{(2)}(\omega)]$  of (a) Zn-PoBe, (b) Zn-PoAz, (c) Zn-PoAzD, (d) Zn-PoAzN, (e) Zn-PoAzNN and (f) Zn-PoAzBN into 2-bands and 3-bands terms.

**Table S1** Electronic properties of selected systems predicted with HLE17 and PBE.

HLE17(PBE)	$E_{\text{Fermi}}/\text{eV}$	$E_{\text{VBM}}/\text{eV}$	$E_{\text{CBM}}/\text{eV}$	$E_{\text{gap}}/\text{eV}$	$E_{\text{scissor}}/\text{eV}$
PoBeD	-5.02 (-3.98)	-6.51 (-3.98)	-4.91 (-2.53)	1.60 (1.45)	0.15
PoBeN	-5.84 (-3.98)	-6.49 (-3.98)	-5.26 (-2.89)	1.23 (1.09)	0.14
PoBeNN	-6.22 (-3.92)	-6.43 (-3.92)	-5.84 (-3.42)	0.59 (0.50)	0.09
PoBeBN	-6.06 (-3.81)	-6.31 (-3.81)	-5.43 (-3.06)	0.88 (0.75)	0.13
Po2Az	-6.20 (-4.06)	-6.62 (-4.12)	-5.38 (-3.03)	1.24 (1.09)	0.15
Po2AzD	-5.47 (-4.10)	-6.58 (-4.09)	-5.46 (-3.12)	1.12 (0.97)	0.15
Po2AzNN	-5.58 (-4.17)	-6.65 (-4.17)	-6.10 (-3.70)	0.55 (0.47)	0.08
Po2AzBN	-5.55 (-4.22)	-6.70 (-4.22)	-5.45 (-3.12)	1.26 (1.10)	0.16
Zn-PoBe	-5.79 (-3.12)	-6.21 (-3.72)	-4.93 (-2.55)	1.28 (1.17)	0.11
Zn-PoAz	-6.10 (-3.34)	-6.58 (-4.08)	-4.94 (-2.59)	1.64 (1.49)	0.15
Zn-PoAzD	-6.30 (-3.44)	-6.62 (-4.14)	-5.08 (-2.74)	1.55 (1.40)	0.15
Zn-PoAzN	-5.89 (-3.52)	-6.45 (-3.98)	-5.41 (-3.05)	1.05 (0.93)	0.12
Zn-PoAzNN	-6.35 (-3.72)	-6.80 (-4.27)	-5.56 (-3.19)	1.24 (1.09)	0.15
Zn-PoAzBN	-5.52 (-3.49)	-6.38 (-3.95)	-5.36 (-3.03)	1.01 (0.92)	0.09
Zn-Po2Az	-6.32 (-3.52)	-6.65 (-4.17)	-5.21 (-2.88)	1.45 (1.29)	0.16
Zn-Po2AzD	-6.09 (-3.65)	-6.40 (-3.95)	-5.66 (-3.31)	0.74 (0.64)	0.10
Zn-Po2AzNN	-6.58 (-3.95)	-6.61 (-4.16)	-6.02 (-3.64)	0.60 (0.52)	0.08
Zn-Po2AzBN	-6.45 (-3.75)	-6.61 (-4.15)	-5.64 (-3.30)	0.97 (0.86)	0.11

Note:  $E_{\text{Fermi}}$  is the position at which the Fermi energy level is located;  $E_{\text{VBM}}$  and  $E_{\text{CBM}}$  denote the top of the valence band and the bottom of the conduction band, respectively;  $E_{\text{gap}}$  is the band gap ( $E_{\text{gap}} = E_{\text{CBM}} - E_{\text{VBM}}$ );  $E_{\text{scissor}}$  is the scissor correction ( $E_{\text{scissor}} = E_{\text{HLE17}} - E_{\text{PBE}}$ ).

**Table S2**  $\chi_{ijk}^{(2)}$  along the x-direction at static limit (in pm/V).

materials	$\chi_{xxx}^{(2)}(0)$	$\chi_{xxy}^{(2)}(0)$	$\chi_{xxz}^{(2)}(0)$	$\chi_{xyx}^{(2)}(0)$	$\chi_{xyy}^{(2)}(0)$	$\chi_{xyz}^{(2)}(0)$	$\chi_{xzx}^{(2)}(0)$	$\chi_{xzy}^{(2)}(0)$	$\chi_{xzz}^{(2)}(0)$
PoBe	0.42	2.59	0.10	2.59	1.54	0.08	0.10	0.08	0.11
PoBeD	0.06	0.02	0.03	0.02	0.02	0.00	0.03	0.00	0.00
PoBeN	0.33	0.07	0.07	0.69	0.11	0.07	0.07	0.07	0.07
PoBeBN	0.21	1.69	0.05	1.69	2.41	0.05	0.05	0.05	0.03
PoAz	0.80	0.10	0.41	0.10	2.24	0.15	0.41	0.15	0.04
PoAzD	1.02	0.23	0.18	0.23	0.09	0.08	0.18	0.08	0.07
PoAzN	4.08	2.17	1.15	2.17	1.26	0.16	1.15	0.16	0.35
PoAzNN	13.92	28.31	2.55	28.31	45.42	0.67	2.55	0.67	0.65
PoAzBN	5.34	2.98	40.44	2.98	1.16	0.23	0.44	0.23	0.23
Po2Az	2.67	0.84	0.12	0.84	0.15	0.01	0.12	0.01	0.01
Po2AzD	3.15	0.35	0.13	0.35	0.54	0.07	0.13	0.07	0.03
Po2AzN	4.63	0.47	0.13	0.47	0.09	0.06	0.13	0.06	0.09
Po2AzBN	1.53	0.19	0.10	0.19	0.46	0.08	0.10	0.08	0.05
Zn-PoBe	0.40	2.52	0.02	2.52	1.33	0.10	0.02	0.10	0.11
Zn-PoAz	0.44	0.05	0.01	0.05	0.10	0.02	0.013	0.02	0.06
Zn-PoAzD	0.95	0.18	0.19	0.18	0.18	0.08	0.19	0.08	0.74
Zn-PoAzN	3.03	1.66	0.94	1.66	1.26	0.16	0.94	0.16	0.25
Zn-PoAzNN	0.50	0.83	0.66	0.83	0.68	0.35	0.66	0.04	0.04
Zn-PoAzBN	3.12	1.63	0.44	1.63	2.04	0.28	0.44	0.28	0.24
Zn-Po2Az	2.02	0.22	0.07	0.22	0.10	0.05	0.07	0.05	0.08
Zn-Po2AzN	4.68	1.76	0.08	1.76	0.20	0.12	0.08	0.12	0.19
Zn-Po2AzBN	0.69	0.34	0.53	0.34	3.90	0.20	0.53	0.20	0.00

**Table S3**  $\chi_{ijk}^{(2)}$  along the  $y$ -direction at static limit (in pm/V).

materials	$\chi_{yxx}^{(2)}$	$\chi_{yxy}^{(2)}$	$\chi_{yxz}^{(2)}$	$\chi_{yyx}^{(2)}$	$\chi_{yyy}^{(2)}$	$\chi_{yyz}^{(2)}$	$\chi_{yzx}^{(2)}$	$\chi_{yzy}^{(2)}$	$\chi_{yzz}^{(2)}$
PoBe	0.99	2.66	0.11	2.66	0.67	0.07	0.11	0.07	0.11
PoBeD	0.02	0.04	0.01	0.04	0.00	0.00	0.01	0.00	0.01
PoBeN	0.69	0.18	0.30	0.18	0.88	0.08	0.30	0.08	0.01
PoBeBN	4.19	1.62	0.41	1.62	0.59	0.31	0.41	0.31	0.44
PoAz	1.55	1.84	0.02	1.84	0.90	0.05	0.02	0.05	0.08
PoAzD	0.11	0.07	0.06	0.07	0.80	0.03	0.06	0.03	0.04
PoAzN	0.66	3.58	0.20	3.58	5.75	0.11	0.20	0.11	0.35
PoAzNN	40.98	34.02	0.67	34.02	14.27	0.54	0.67	0.54	0.54
PoAzBN	0.96	3.12	0.23	3.12	5.58	0.35	0.23	0.35	0.23
Po2Az	0.54	0.54	0.01	0.54	3.08	0.12	0.01	0.12	0.03
Po2AzD	0.04	0.40	0.12	0.40	2.21	0.09	0.12	0.09	0.08
Po2AzN	0.15	1.05	0.06	1.05	6.04	1.00	0.06	1.00	0.10
Po2AzBN	0.30	0.14	0.07	0.14	1.86	0.21	0.07	0.21	0.05
Zn-PoBe	1.17	2.43	0.07	2.43	0.53	0.02	0.07	0.02	0.10
Zn-PoAz	0.07	0.02	0.03	0.02	0.57	0.03	0.03	0.03	0.05
Zn-PoAzD	0.16	0.08	0.06	0.08	0.97	0.07	0.06	0.07	0.06
Zn-PoAzN	0.99	2.06	0.17	2.06	4.42	0.15	0.17	0.15	0.28
Zn-PoAzNN	0.69	0.30	0.07	0.30	0.67	0.13	0.07	0.13	0.10
Zn-PoAzBN	2.31	1.68	0.27	1.68	3.51	0.27	0.27	0.27	0.23
Zn-Po2Az	0.01	0.10	0.00	0.10	2.31	0.02	0.00	0.02	0.17
Zn-Po2AzN	0.30	1.26	0.10	1.26	7.88	1.30	0.10	1.30	0.19
Zn-Po2AzBN	2.09	3.19	0.01	3.19	2.52	0.28	0.01	0.28	0.05

**Table S4**  $\chi_{ijk}^{(2)}$  along the z-direction at static limit (in pm/V).

materials	$\chi_{zxx}^{(2)}(0)$	$\chi_{zxy}^{(2)}(0)$	$\chi_{zxz}^{(2)}(0)$	$\chi_{zyx}^{(2)}(0)$	$\chi_{zyy}^{(2)}(0)$	$\chi_{zyz}^{(2)}(0)$	$\chi_{zzx}^{(2)}(0)$	$\chi_{zzy}^{(2)}(0)$	$\chi_{zzz}^{(2)}(0)$
PoBe	0.22	0.09	0.01	0.09	0.23	0.01	0.01	0.01	0.02
PoBeD	0.01	0.03	0.00	0.02	0.00	0.00	0.00	0.00	0.00
PoBeN	0.15	0.08	0.00	0.08	0.12	0.01	0.00	0.01	0.00
PoBeBN	0.12	0.06	0.02	0.06	0.23	0.09	0.02	0.09	0.01
PoAz	0.10	0.06	0.05	0.06	0.08	0.03	0.05	0.03	0.01
PoAzD	0.02	0.05	0.05	0.05	0.08	0.04	0.05	0.04	0.02
PoAzN	0.19	0.16	0.11	0.16	0.01	0.09	0.11	0.09	0.02
PoAzNN	0.95	0.01	0.14	0.01	0.36	0.13	0.14	0.13	0.01
PoAzBN	0.17	0.03	0.07	0.03	0.17	0.07	0.07	0.07	0.01
Po2Az	0.07	0.00	0.07	0.00	0.05	0.08	0.07	0.08	0.00
Po2AzD	0.02	0.00	0.07	0.00	0.03	0.10	0.07	0.10	0.00
Po2AzN	0.02	0.01	0.10	0.01	0.34	0.15	0.10	0.15	0.03
Po2AzBN	0.06	0.00	0.10	0.00	0.10	0.11	0.10	0.11	0.00
Zn-PoBe	0.22	0.07	0.01	0.07	0.24	0.01	0.01	0.01	0.01
Zn-PoAz	0.01	0.00	0.05	0.00	0.01	0.04	0.05	0.04	0.01
Zn-PoAzD	0.03	0.05	0.05	0.05	0.09	0.04	0.05	0.04	0.01
Zn-PoAzN	0.06	0.18	0.10	0.18	0.02	0.09	0.10	0.09	0.01
Zn-PoAzNN	0.12	0.04	0.03	0.04	0.07	0.01	0.03	0.01	0.01
Zn-PoAzBN	0.07	0.02	0.07	0.02	0.06	0.07	0.07	0.07	0.00
Zn-Po2Az	0.03	0.02	0.09	0.02	0.01	0.08	0.09	0.08	0.00
Zn-Po2AzN	0.03	0.05	0.10	0.05	0.48	0.15	0.10	0.15	0.02
Zn-Po2AzBN	0.32	0.12	0.02	0.12	0.00	0.09	0.02	0.09	0.01

**Table S5** The electronic properties of molecules predicted with B3LYP/6-31G (d, p).

Compound	$\Delta E_{OS-CS}$	$\Delta E_{T-CS}$	$\langle S^2 \rangle$	LVF	$E_{HOMO}$	$E_{LUMO}$	$E_{gap}$	$D_g$
PoBe	0.00	36.65	0.00	8.11	-4.92	-2.21	2.71	0.03
PoBeD	0.00	30.34	0.00	9.2	-4.92	-2.24	2.68	0.31
PoBeN	0.00	30.21	0.00	8.98	-5.16	-2.47	2.69	5.46
PoBeNN	0.00	30.97	0.00	9.27	-5.23	-2.55	2.68	6.49
PoBeBN	0.00	41.57	0.00	9.44	-4.89	-2.20	2.69	0.45
PoAz	0.00	51.77	0.00	9.40	-5.06	-2.37	2.69	2.23
PoAzD	0.00	36.57	0.00	8.11	-5.03	-2.41	2.61	2.01
PoAzN	0.00	36.76	0.00	8.27	-5.19	-2.63	2.56	5.92
PoAzNN	0.00	25.27	0.00	8.26	-5.27	-2.77	2.50	7.81
PoAzBN	0.00	36.77	0.00	8.32	-5.17	-2.57	2.60	4.62
Po2Az	0.03	37.24	0.00	6.90	-4.92	-2.45	2.47	4.05
Po2AzD	0.00	29.40	0.00	6.64	-4.90	-2.45	2.45	3.81
Po2AzN	0.00	37.26	0.00	6.60	-4.99	-2.54	2.45	6.45
Po2AzNN	0.00	21.16	0.00	6.68	-5.17	-2.77	2.39	11.78
Po2AzBN	0.00	27.84	0.00	6.50	-5.04	-2.56	2.48	6.63
Zn-Po2AzN	0.00	34.57	0.00	6.59	-5.05	-2.46	2.59	6.18
Zn-Po2AzBN	0.00	34.45	0.00	6.50	-5.11	-2.47	2.64	6.62

$\Delta E_{OS-CS}$  and  $\Delta E_{T-CS}$  are the relative electronic energy differences between open-shell (OS) singlet or triplet (T) and closed-shell (CS) singlet (CS is taken as reference) (in kcal/mol); LVF is the lowest vibrational frequency (in  $cm^{-1}$ );  $E_{gap}$  is the energy gap between HOMO and LUMO (in eV);  $\langle S^2 \rangle$  is the spin contamination of open-shell singlet obtained at B3LYP/6-31G (d, p) level;  $D_g$  is the ground state dipole (in Debye).